Am J Physiol Heart Circ Physiol 311: H168–H176, 2016.
First published May 6, 2016; doi:10.1152/ajpheart.00132.2016.

The endothelial glycocalyx promotes homogenous blood flow distribution within the microvasculature

P. Mason McClatchey,[1,2,3] Michal Schafer,[3,4] Kendall S. Hunter,[3,4] and Jane E. B. Reusch[1,2,3,5]

[1]*Division of Endocrinology, University of Colorado Anschutz Medical Campus, Aurora, Colorado;* [2]*Department of Medicine, Denver Veterans Affairs Medical Center, Denver, Colorado;* [3]*Department of Bioengineering, University of Colorado Anschutz Medical Campus, Aurora, Colorado;* [4]*Division of Cardiology, Department of Pediatrics, Children's Hospital Colorado, Aurora, Colorado; and* [5]*Center for Women's Health Research, University of Colorado School of Medicine, Aurora, Colorado*

Submitted 12 February 2016; accepted in final form 3 May 2016

McClatchey PM, Schafer M, Hunter KS, Reusch JE. The endothelial glycocalyx promotes homogenous blood flow distribution within the microvasculature. *Am J Physiol Heart Circ Physiol* 311: H168–H176, 2016. First published May 6, 2016; doi:10.1152/ajpheart.00132.2016.—Many common diseases involve impaired tissue perfusion, and heterogeneous distribution of blood flow in the microvasculature contributes to this pathology. The physiological mechanisms regulating homogeneity/heterogeneity of microvascular perfusion are presently unknown. Using established empirical formulations for blood viscosity modeling in vivo (blood vessels) and in vitro (glass tubes), we showed that the in vivo formulation predicts more homogenous perfusion of microvascular networks at the arteriolar and capillary levels. Next, we showed that the more homogeneous blood flow under simulated in vivo conditions can be explained by changes in red blood cell interactions with the vessel wall. Finally, we demonstrated that the presence of a space-filling, semipermeable layer (such as the endothelial glycocalyx) at the vessel wall can account for the changes of red blood cell interactions with the vessel wall that promote homogenous microvascular perfusion. Collectively, our results indicate that the mechanical properties of the endothelial glycocalyx promote homogeneous microvascular perfusion. Preservation or restoration of normal glycocalyx properties may be a viable strategy for improving tissue perfusion in a variety of diseases.

glycocalyx; microvascular perfusion; perfusion heterogeneity; oxygen delivery

NEW & NOTEWORTHY

This study identifies a microfluidic-based mechanism for the abnormal distribution of microvascular blood flow observed under conditions of glycocalyx degradation and suggests a causal role for glycocalyx degradation in impaired tissue perfusion and oxygenation in several nominally unrelated disease states.

MICROVASCULAR PERFUSION HETEROGENEITY (unequal distribution of microvascular blood flow within target tissues) has been observed in a wide variety of disease states, including sepsis (27), aging (28), type 2 diabetes (18), and chronic heart failure (46). In each of these disease states, the capacity for aerobic exercise is reduced (5, 15, 48, 59). Many mechanisms have been proposed to contribute to exercise impairment in these conditions, including loss of muscle mass (15), reduced nutritive blood flow (59), abdominal obesity (35), increased circulating inflammatory markers (26), and endothelial dysfunction (19). It is reasonable to suggest that microvascular perfusion heterogeneity itself might contribute to reductions whole body oxygen uptake, based on both empirical (17, 23) and theoretical (22, 36) data demonstrating that microvascular perfusion heterogeneity limits oxygen extraction independently of total blood flow. Perfusion heterogeneity is a plausible mechanism for impaired oxygenation in virtually any tissue, given that the mechanism of impairment (namely, that some capillaries are underperfused and deliver less oxygen, whereas others are overperfused and effectively saturate their capacity for oxygen delivery) is not tissue specific.

One potential cause of disease-related microvascular perfusion heterogeneity is degradation of the endothelial glycocalyx and subsequent changes in the determinants of effective blood viscosity. The glycocalyx is a space-filling (~1 μm wide) semipermeable layer of glycosaminoglycans and proteoglycans lining the luminal surface of blood vessels. Experimental glycocalyx degradation causes microvascular perfusion heterogeneity, thus reducing the number of capillaries supporting red blood cell (RBC) flux (10, 12, 63) and decreasing oxygen utilization (6, 11). Precisely these same derangements in microvascular perfusion are observed in sepsis (27), type 1 diabetes (25), type 2 diabetes (37), and heart failure (49), along with findings of glycocalyx perturbation (7, 8, 34, 58) and oxygen utilization limitations (5, 15, 48, 59). It seems likely, then, that glycocalyx degradation could cause impairments in tissue oxygenation secondary to microvascular perfusion heterogeneity.

The link between disease-mediated glycocalyx degradation and microvascular perfusion heterogeneity has not been fully explained. Hints of a unifying mechanism can be found in rheological studies of blood viscosity. Pries et al. (41, 45) observed that microvascular blood viscosity in vivo (measurements performed in blood vessels) is far greater than that observed in vitro (measurements performed in glass tubes), particularly at the precapillary and capillary levels. This discrepancy in viscosity can be mathematically accounted for by the mechanical effects of a space-filling glycocalyx at the endothelial surface (42).

Several distinct lines of historical data have informed our understanding of the relationship between glycocalyx properties and microvascular perfusion independently of total blood flow (see the schema in Fig. 1). Empirical formulations of blood viscosity (41, 45) and their application microvascular perfusion simulations (44) indicate that the distribution of blood flow at microvascular bifurcations is determined by both blood viscosity effects and differences in downstream resistance. The interactions between vessel diameter and effective

Address for reprint requests and other correspondence: J. E. B. Reusch, 12801 E. 17th Ave, MS 8106, Aurora, CO 80045 (e-mail: jane.reusch@ucdenver.edu).

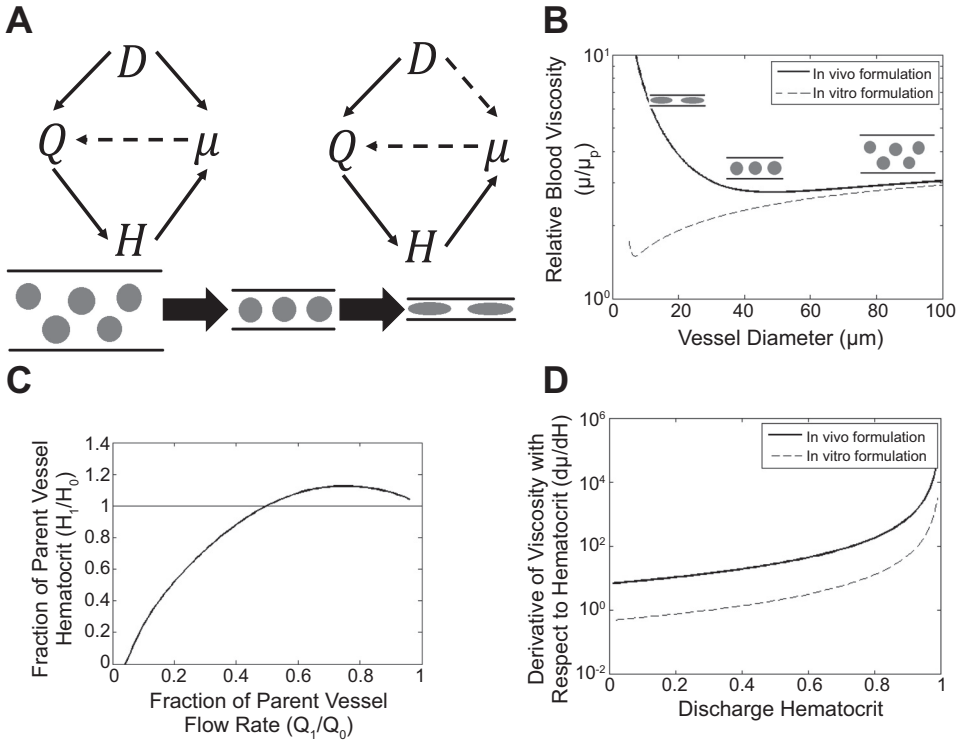

Fig. 1. Schema of established determinants of microvascular blood flow distribution based on the literature. *A*: relationships between parameters influencing microvascular blood flow distribution during the transition from multifile to single file flow (*left*) and during red blood cell (RBC) deformation (*right*). Causal increases (i.e., increases in *A* cause increases in *B*) are indicated by solid arrows, whereas causal decreases are indicated by dashed arrows. Here, *D* is vessel diameter, *Q* is flow rate, *H* is hematocrit, and μ is viscosity. *B*: blood viscosity (*y*-axis) changes with changing vessel diameter (*x*-axis) both in vivo and in vitro. In vitro, increasing vessel diameter increases microvascular blood viscosity at all physiologically relevant vessel diameters. In vivo, increasing vessel diameter decreases blood viscosity at the capillary and precapillary levels but otherwise increases blood viscosity. *C*: ratio of daughter vessel hematocrit to parent vessel hematocrit (*y*-axis) as a function of the fraction of the parent vessel flow rate received by the daughter vessel (*x*-axis). An idealized bifurcation in which all vessels are 10 μm in diameter and feed hematocrit of 0.45 was simulated to create this graph. *D*: derivative of microvascular blood viscosity (*y*-axis) with respect to vessel hematocrit (*x*-axis). Although increases in hematocrit increase blood viscosity both in vivo and in vitro, this effect is much stronger in vivo (41, 45).

blood viscosity (decreasing diameter decreases viscosity in larger microvessels and increases viscosity in smaller microvessels) and between hematocrit and viscosity (increasing hematocrit increases viscosity) introduce additional determinants of flow distribution within the microcirculation compared with a simple Newtonian fluid (Fig. 1*A*). Vessel diameter has a complex interaction with effective blood viscosity in microvessels due the particulate nature of blood (Fig. 1*B*). In larger microvessels (10s to 100s of micrometers in diameter), decreasing vessel diameter is associated with decreasing viscosity as RBC flow gradually shifts from multifile to single file (i.e., shear thinning) (43). In smaller vessels (i.e., less than ~30 μm in diameter), decreasing vessel diameter is associated with increasing viscosity as RBC deformation increases with decreasing vessel diameter. The shift from shear thinning to RBC deformation occurs at a larger vessel diameter in vivo relative to in vitro. Increasing hematocrit (fraction of vessel lumen volume filled by RBCs) is associated with increased viscosity regardless of scale, and this effect is most pronounced in the smallest blood vessels. Hematocrit is increased in the higher flow branch of a microvascular bifurcation and decreased in the lower flow branch (40) (Fig. 1*C*), providing a negative feedback mechanism to regulate flow partition (increased flow increases hematocrit, thus increasing viscosity and limiting the increase in flow). The dependence of blood viscosity on hematocrit is nearly an order of magnitude greater in vivo than in vitro (Fig. 1*D*), indicating that unequal distribution of RBCs would incur a greater energy cost in vivo than in vitro.

In this study, we used mathematical models of blood viscosity and microvascular rheology to simulate the impact of differences in microvascular structure, blood viscosity behaviors, and glycocalyx properties on the distribution of blood flow within the microcirculation. We use this simulation method to predict the impact of glycocalyx modification (common in aging and disease) upon tissue perfusion. These data support the hypothesis that the glycocalyx is a central regulator of tissue perfusion and oxygenation independently of blood flow redistribution to match metabolic demand. This finding has important implications for tissue perfusion in health and disease, as the glycocalyx is highly dynamic and presents a novel therapeutic target.

METHODS

Simulation of blood flow and RBC distribution. The methods of Pries et al. (44) were used for the simulation of blood flow and RBC distribution. In this technique, distribution of RBCs and whole blood (including both RBCs and plasma) at microvascular bifurcations are determined according to an empirical formulation relating RBC distribution to vessel diameters, flow rates, and hematocrit (40). These relationships are shown in *Eqs. 1–5*. Here, FQ_E is fractional RBC flow, FQ_B is fractional blood flow, *logit* is a logistic function defined in *Eq. 1*, X_0 is minimal fractional blood flow to support RBC flux, D_0

is parent vessel diameter, D_1 is the diameter of *daughter vessel 1*, D_2 is the diameter of *daughter vessel 2*, H is parent vessel hematocrit, and A and B are empirically defined scaling parameters.

$$\text{logit}\left(FQ_E\right) = A + B \times \text{logit}\left(\frac{FQ_B - X_O}{1 - 2 \times X_O}\right) \quad (1)$$

$$\text{logit}\left(x\right) = \ln\left(\frac{x}{1-x}\right) \quad (2)$$

$$A = -6.96 \times \frac{\text{In}\left(\frac{D_1}{D_2}\right)}{D_0} \quad (3)$$

$$B = 1 + 6.98 \times \left(\frac{1-H}{D_0}\right) \quad (4)$$

$$X_0 = \frac{0.4}{D_0} \quad (5)$$

Flow distribution was optimized at each bifurcation to ensure total pressure drops across parallel vascular routes were equal to a relative error of $<10^{-6}$. Pressure drops were assessed using established empirical formulations of microvascular blood viscosity in vitro (glass tubes) (41) and in vivo (blood vessels) (45) to assess the contributions of the endothelium to regulation of blood flow distribution in vivo. These empirical microvascular blood viscosity relationships are shown in *Eqs. 6–8* (in vivo) and *Eqs. 6*, *9*, and *10* (in vitro). Here, μ_{vivo} is in vivo blood viscosity at hematocrit H, μ_p is plasma viscosity, $\mu_{45,vivo}$ is in vivo blood viscosity at a hematocrit of 0.45, C is an empirical scaling factor that modulates the interplay between vessel diameter and hematocrit sensitivity of blood viscosity, D is vessel diameter (in μm), μ_{vitro} is in vitro blood viscosity at hematocrit H, and $\mu_{45,vitro}$ is in vitro blood viscosity at a hematocrit of 0.45.

$$C = \left(0.8 + e^{-0.075\times D}\right) \times \left(-1 + \frac{1}{1 + 10^{-11} \times D^{12}}\right) + \frac{1}{1 + 10^{-11} \times D^{12}} \quad (6)$$

$$\mu_{vivo} = \mu_p \times \left[\left(1 + \mu_{45,vivo} - 1\right) \times \frac{\left(1-H\right)^C - 1}{\left(1-0.45\right)^C - 1} \times \left(\frac{D}{D-1.1}\right)^2\right] \times \left(\frac{D}{D-1.1}\right)^2 \quad (7)$$

$$\mu_{45,vivo} = 6 \times e^{-0.085\times D} + 3.2 - 2.44 \times e^{-0.06\times D^{0.645}} \quad (8)$$

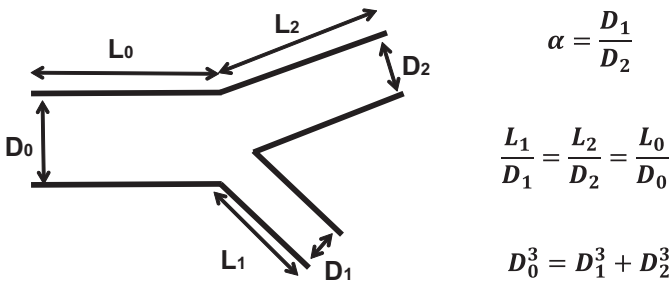

Fig. 2. Parameters used to create idealized arteriolar trees. Each parent vessel terminates at a bifurcation of two smaller vessels. At each bifurcation, the parent vessel is denoted by subscript 0, the smaller daughter vessel is denoted by subscript 1, and the larger daughter vessel is denoted by subscript 2. Bifurcation asymmetry parameter α is defined in terms of the relative diameters of the daughter vessels. The length-to-diameter ratio is held constant across vessel generations. Murray's cube law (33) was used to define the scaling of successive vessel generations. Here, D is vessel diameter, L is vessel length, and the subscripts denote the vessel segments.

$$\mu_{vitro} = \mu_p \times \left(1 + \mu_{45,vitro} - 1 \times \frac{\left(1-H\right)^C - 1}{\left(1-0.45\right)^C - 1}\right) \quad (9)$$

$$\mu_{45,vitro} = 220 \times e^{-1.3\times D} + 3.2 - 2.44 \times e^{-0.06\times D^{0.645}} \quad (10)$$

Because heterogeneity of transit times (time spent within the microvasculature) has been shown to be the basis for impaired oxygen transport with heterogeneity of microvascular perfusion (22, 36), we used transit time heterogeneity (as assessed by the SD-to-mean ratio) at both terminal arteriole [consistent with theoretical analyses (22, 36)] and whole network [consistent with animal studies using radiolabeled plasma (9, 18)] levels to assess microvascular blood flow distribution in our simulations.

Idealized arteriolar branching structure for network perfusion simulations. An idealized arteriolar tree consisting of seven successive vessel generations was used for all network perfusion simulations. A vessel diameter of 50 μm at the first vessel generation was used for all simulations, resulting in a range of vessel diameters consistent with precapillary arterioles. A maximal diameter of 50 μm was chosen because in vivo and in vitro blood viscosity behaviors begin to diverge at this scale (see Fig. 1*B*). Terminal vessel diameters varied according to the parameter values used but were centered on an average of 12.5 μm. Each vessel terminated at a bifurcation characterized by the parameters shown in Fig. 2. The parameter $\alpha = D_1/D_2$ was used to define asymmetry in daughter vessel diameters at each bifurcation. Murray's cube law (33) was used to determine the scale of downstream vessels at each bifurcation, and the resulting vascular tree was consistent with the L-system fractal formalism of Zamir et al. (60). Although more sophisticated formulations of microvascular branching structure have been developed (4, 21, 53), the mathematical rules used in this study have been validated as reasonable approximations of microvascular structure in a variety of tissues (60, 61) and allow for straightforward assessment of the interactions between blood viscosity formulations, microvascular structure, and the resulting distribution of microvascular blood flow.

Simulation of glycocalyx influences on luminal plasma velocity profiles. Whereas the analyses described above in *Simulation of blood flow and RBC distribution* and *Idealized arteriolar branching structure for network perfusion simulations* aimed to determine differences in perfusion predicted from in vivo and in vitro measurements, the analysis described here aimed to determine whether these perfusion differences can be accounted for by the mechanical influences of the endothelial glycocalyx. The mechanical influences of the endothelial glycocalyx derive from both its space-filling and semipermeable nature. To assess the effects such a layer at the vessel wall on the sensitivity of blood viscosity to hematocrit, flow velocity profiles were developed in vessels containing an idealized glycocalyx were simulated using a radial, one-dimensional finite difference approach (see *Influence of glycocalyx properties on the determinants of blood viscosity* below for examples). Simulations were performed in Matlab 2013. The glycocalyx was assumed to have a fixed width of w (in μm) and a fixed Darcy permeability of K (in Darcy units). A fixed lift distance of 100 nm between the glycocalyx and RBC membrane was used for these simulations. Fully developed flow and a no-slip boundary condition were assumed for all simulations. Velocities at each radial node were adjusted to achieve a uniform (relative error of $<10^{-10}$), nonzero pressure drop across a length-normalized capillary segment, as assessed using Eqs. *11* and *12*. A radial resolution of 12.5 nm was used for all simulations. Each simulation was repeated twice: once assuming plasma only (*Eq. 11*) and once assuming a RBC in the vessel lumen (*Eq. 12*). Here, L is vessel length, ΔP is the change in pressure, r is the radial position within the capillary, R is the radius of the capillary, R_C is the radius of the RBC, and V is velocity. These physical parameters were closely based on those used in previous studies simulating the effect of the glycocalyx on luminal flow profiles (14, 50, 51).

$$\frac{\Delta P}{L} = \begin{Bmatrix} 2 \times \pi \times r \times \mu \times \frac{dV}{dr}(r) & r < R - w \\ 2 \times \pi \times r \times \mu \times \frac{dV}{dr}(r) + \left(\frac{\mu}{K}\right) \times \int_{R-w}^{r} 2 \times \pi \times r \times V * dr & r \geq R - 2 \end{Bmatrix} \quad (11)$$

$$\frac{\Delta P}{L} = \begin{Bmatrix} \frac{\Delta P}{L} & r < R_c \\ 2 \times \pi \times r \times \mu \times \frac{dV}{dr}(r) & R_c \leq r < R - 2 \\ 2 \times \pi \times r \times \mu \times \frac{dV}{dr}(r) + \left(\frac{\mu}{K}\right) \times \int_{R-w}^{r} 2 \times \pi \times r \times V \times dr & r \geq R - 2 \end{Bmatrix} \quad (12)$$

Empirical studies of microvascular rheology have demonstrated that effective microvascular blood viscosity depends heavily on hematocrit and diameter and that the relative importance of these sensitivities is different in vivo and in vitro (41, 45). Drawing from the results of Secomb et al. (50), the sensitivity of microvascular blood viscosity to hematocrit can be characterized for discharge hematocrits (hematocrit of effluent blood in a microvessel) of less than ~0.6 based on differences in flow resistance with and without a RBC in the vessel lumen, as shown in *Eq. 13*. Here, μ_e is effective blood viscosity, μ_p is plasma viscosity, Hct is hematocrit, and K_T is the hematocrit sensitivity of blood viscosity.

$$\mu_e = \mu_p \times (1 + K_T \times \mathrm{Hct}) \quad (13)$$

RESULTS

Flow distribution in branching arteriolar networks. Observation of arteriolar branching architecture in vivo reveals that arterioles often bifurcate into a larger vessel (usually serving a larger downstream capillary bed) and a smaller vessel (usually serving a smaller downstream capillary bed) (60, 61). To assess the effects of asymmetric bifurcations in the arteriolar tree on tissue perfusion, we first modeled flow in idealized arteriolar networks with seven successive vessel generations, a constant length-to-diameter ratio, and a fixed ratio of smaller daughter vessel diameter to larger daughter vessel diameter (Fig. 3*A*), as

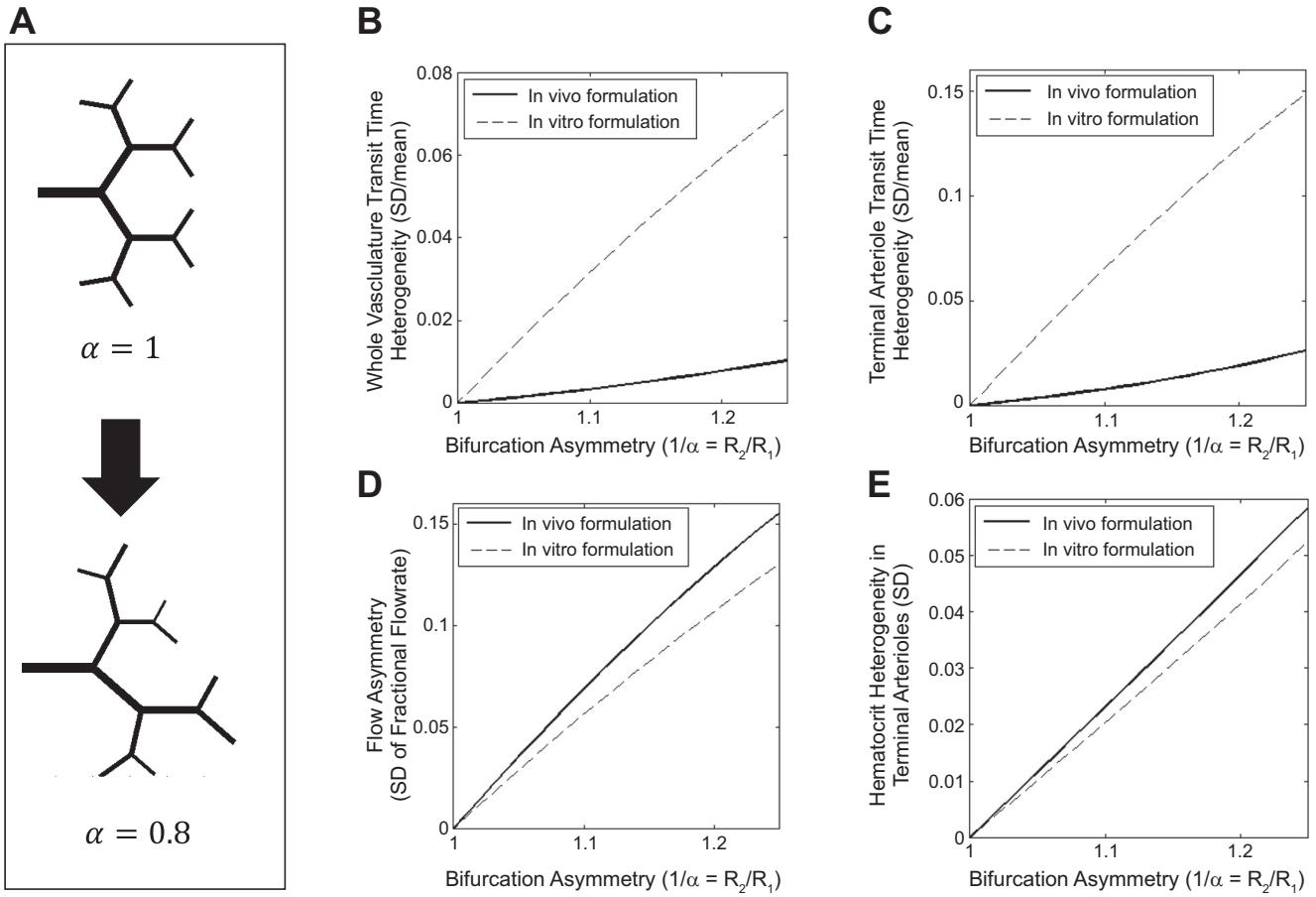

Fig. 3. Influences of microvascular blood viscosity on microvascular perfusion heterogeneity in a simulated arteriolar tree. *A*: schematic of the idealized arteriolar networks obtained by varying the bifurcation parameter α (see Fig. 1). All arteriolar networks simulated consisted of seven successive vessel generations with fractal vessel architecture. *B*: heterogeneity (SD/mean) of the whole network transit time is reduced in vivo (blood vessels) compared with in vitro (glass tubes) for all values of α. *C*: heterogeneity (SD/mean) of the terminal vessel transit time is reduced in vivo compared with in vitro for all values of α. *D*: SD of the fractional daughter vessel flow rate is subtly increased in vivo compared with in vitro for all values of α. *E*: SD of the terminal vessel hematocrit is subtly increased in vivo compared with in vitro for all values of α.

detailed in *Idealized arteriolar branching structure for network perfusion simulations*.

Increasing bifurcation asymmetry results in increased heterogeneity of vascular transit times (as assessed by the SD-to-mean ratio) at both the whole vasculature (Fig. 3*B*) and single vessel (Fig. 3*C*) levels. In both cases, the increase in transit time heterogeneity is far more pronounced using an empirical in vitro blood viscosity formulation than using an empirical in vivo blood viscosity formulation. These results are in contrast to the effects of bifurcation asymmetry on flow asymmetry (Fig. 3*D*, assessed as the SD of fractional flow rate at each bifurcation) and terminal vessel hematocrit heterogeneity (Fig. 3*E*, assessed as the SD of hematocrit). According to these metrics, increases in flow and hematocrit heterogeneity are more pronounced using an empirical in vivo blood viscosity formulation than using an empirical in vitro blood viscosity formulation. The apparent divergence of transit time and flow heterogeneity results stems from the fact that larger upstream vessels feed a larger volume of downstream blood vessels (see Fig. 3*A*). Because transit time is determined by the ratio of luminal volume to flow rate, a more pronounced asymmetry of flow distribution at the single bifurcation level with in vivo blood viscosity (Fig. 3*D*) would be expected to result in reduced heterogeneity of vascular transit times under the same conditions (Fig. 3*B*). These results indicate that the microvascular perfusion heterogeneity caused by vessel diameter effects at the arteriolar level would be more pronounced in glass tubes than in blood vessels and that this effect is a result of the increased effective blood viscosity in precapillary arterioles in vivo (Fig. 1*B*).

Flow distribution at an idealized capillary bifurcation. Observation of capillary networks in vivo reveals that variations in capillary diameter within a given tissue are typically minor compared with variations in capillary length, glycocalyx dimensions, and other diameter-independent determinants of capillary blood flow (30, 38, 39). To assess the differential effects of empirical blood viscosity formulations based on measurements taken in vivo (blood vessels) and in vitro (glass tubes) on capillary perfusion, we simulated blood flow distribution at an idealized capillary bifurcation consisting of a 6-μm-diameter parent vessel and two 6-μm-diameter daughter vessels with unequal downstream resistances ρ_1 and ρ_2 (Fig. 4*A*). Downstream resistances were multiplied by blood viscosity such that increases in microvessel hematocrit induced increases in downstream resistance. As a result of the increased hematocrit dependence of microvascular blood viscosity in vivo, fractional flow rate at an idealized capillary bifurcation is less dependent on downstream resistances in vivo than in vitro (Fig. 4*B*). As a result of this effect and the relationship between fractional flow rate and downstream hematocrit (Fig. 1*C*), our simulations predict that capillary hematocrits downstream of an idealized bifurcation would be more different using an empirical in vitro blood viscosity formulation than an empirical in vivo blood viscosity formulation (Fig. 4*C*). These results indicate that an increased hematocrit dependence of blood viscosity (Fig. 1*D*) limits microvascular perfusion heterogeneity at the capillary level in blood vessels relative to glass tubes.

Influence of glycocalyx properties on the determinants of blood viscosity. To clarify the contributions of the endothelial glycocalyx specifically (rather than predicting differences in blood flow distribution in blood vessels as opposed to glass tubes), we used a one-dimensional finite difference approach to simulate the influences of glycocalyx permeability and width on the sensitivity of blood viscosity to hematocrit and the

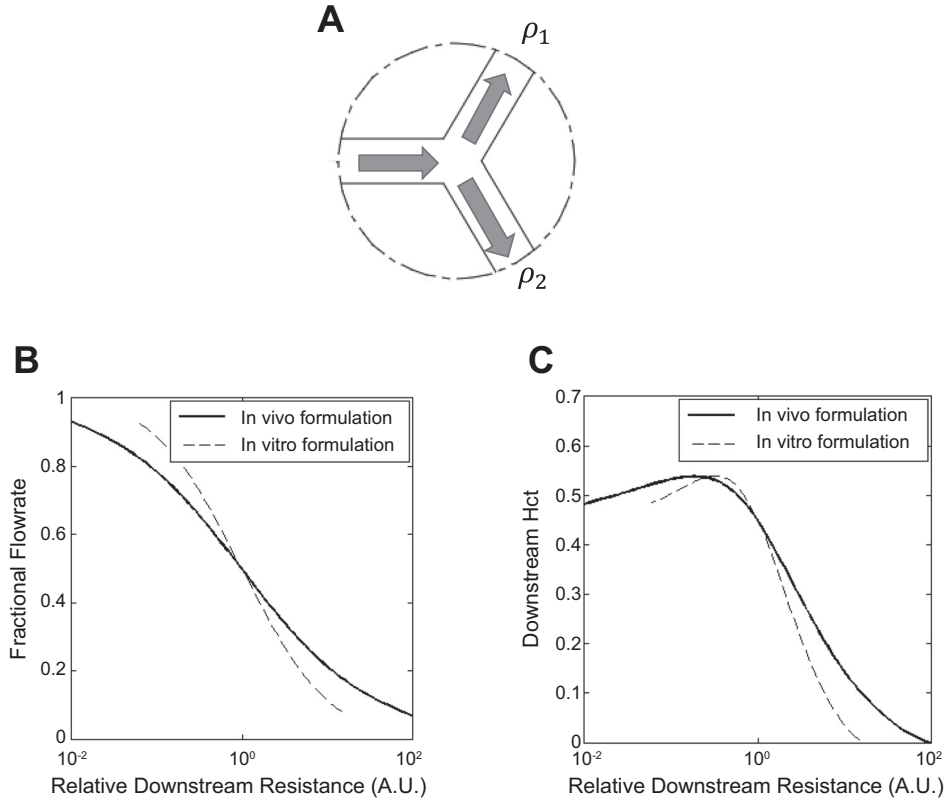

Fig. 4. Influences of microvascular blood viscosity on blood flow distribution at an idealized capillary bifurcation. *A*: schematic of idealized capillary bifurcation. Arrows indicate the direction of flow. Both daughter vessels and the parent vessel are all of identical diameter. Daughter vessels differ only in their resistance to flow distal to the bifurcation (ρ_1 and ρ_2). *B*: fraction of parent vessel flow rate received by *daughter vessel 1* as a function of relative downstream resistance (ρ_1/ρ_2). In vivo blood viscosity behaviors provide a more equal distribution of flow for all values of ρ_1/ρ_2. *C*: fraction of parent vessel hematocrit in *daughter vessel 1* as a function of relative downstream resistance (ρ_1/ρ_2). In vivo blood viscosity behaviors result in less downstream capillary hematocrit heterogeneity for all values of ρ_1/ρ_2.

effective viscosity of blood at the capillary level in isolation of other influences. Drawing from previous studies (14, 50, 51), we elected to test the effects of glycocalyx permeability and width. Flow profiles at near-physiological values of glycocalyx permeability ($K_0 = 10^{-10}$ Darcy) and width (0.75 μm) were consistent with those reported in previous studies (Fig. 5*A*). Note that some of the studies referenced above reported hydraulic resistivity (the inverse of permeability) or water permeability (permeability to water) rather than Darcy permeability per se. Literature values for glycocalyx permeability are largely consistent when presented in similar units.

The sensitivity of microvascular blood viscosity to hematocrit decreases with increasing glycocalyx permeability regardless of glycocalyx width, and this effect is most pronounced at near-physiological values (14, 50, 51, 52, 56) for glycocalyx permeability (Fig. 5*B*). The sensitivity of blood viscosity to hematocrit varies relatively little with glycocalyx width within the range of literature reported values (3, 24, 42, 47, 56). The effective viscosity of blood (hematocrit = 0.45) at the capillary level decreases with increasing glycocalyx permeability, and this effect is further modulated by glycocalyx width (Fig. 5*C*). In total, our results indicate that the sensitivity of blood viscosity to hematocrit is primarily determined primarily by glycocalyx permeability. The effective viscosity of blood in the microcirculation is strongly modulated by both glycocalyx permeability and glycocalyx width.

DISCUSSION

The simulations outlined in this study were performed to clarify the contribution of the endothelial glycocalyx to the regulation of microvascular blood flow distribution. Collectively, our results indicate that the endothelial glycocalyx increases the homogeneity of microvascular perfusion by enhancing interactions between RBCs and the vessel wall within the microcirculation. By comparing flow distributions predicted with empirical in vivo (blood vessels) and in vitro (glass tubes) formulations of blood viscosity in idealized arteriolar trees with unequal downstream diameters at each bifurcation, we show that blood vessels promote homogenous perfusion in branching microvascular networks. By comparing flow distributions predicted with empirical in vivo and in vitro formulations of blood viscosity at an idealized capillary bifurcation, we show that the increasing marginal energy costs associated with cellular flow promotes homogenous perfusion at the capillary level. Finally, by comparing luminal plasma velocity profiles and pressure gradients with and without a RBC in the vessel lumen across a wide range of values for glycocalyx width and permeability, we show that the sensitivity of microvascular blood viscosity to hematocrit at a given vessel diameter is determined primarily by glycocalyx permeability while the increased effective viscosity of blood is strongly influenced by both the width and permeability of the glycocalyx. In total, our simulations suggest that the presence of a semipermeable, space-filling glycocalyx layer in the vessel lumen is sufficient to promote homogeneity of microvascular perfusion by enhancing RBC interactions with the endothelium.

A nontechnical summary of our findings is shown in Fig. 6. Our simulations begin at the precapillary arteriolar level (diameter $<$ 50 μm) and end at the capillary level. Because the majority of the pressure drop in the arterial circulation has already occurred at this point, the redistribution of blood flow to meet metabolic demands occurs upstream of the microvessels considered in this analysis. Oxygen delivery (as opposed to blood flow) may still be modulated by the homogeneity/heterogeneity of blood flow and RBC distribution. At the precapillary arteriolar level, daughter vessel diameters at any

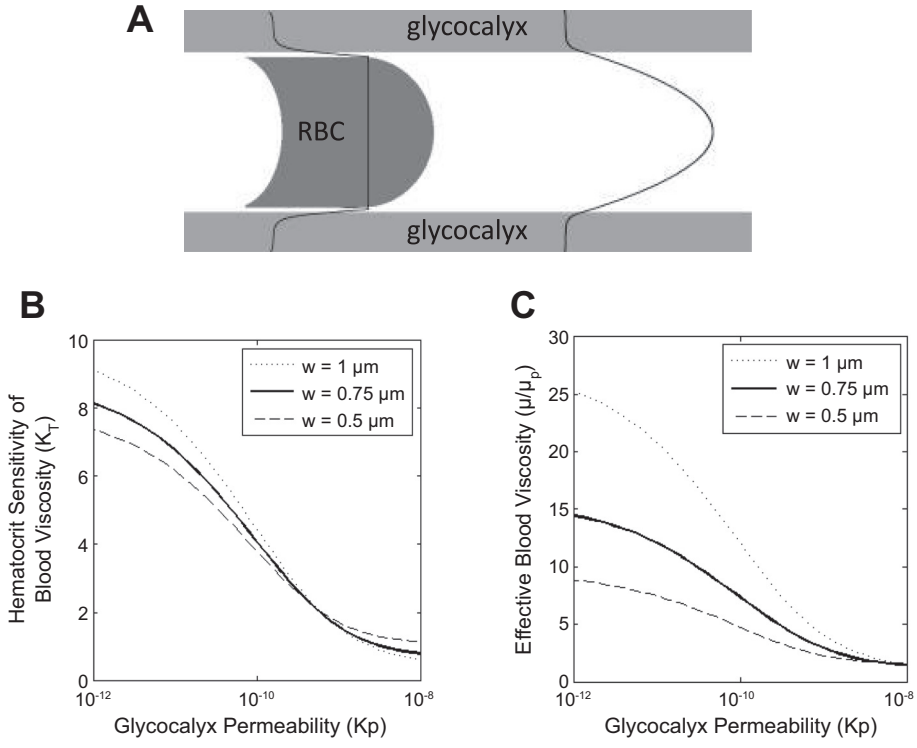

Fig. 5. Effects of glycocalyx properties on the determinants of blood viscosity. *A*: representative velocity profiles within the vessel with and without a RBC in the lumen. Shaded gray areas represent the glycocalyx. Compare with the results of Secomb et al. (50). *B*: sensitivity of microvascular blood viscosity to hematocrit decreases with increasing glycocalyx permeability (Darcy permeability). This effect is influenced little by glycocalyx width. *C*: effective blood viscosity at the capillary level increases with decreasing glycocalyx permeability. This effect is further compounded by the effects of glycocalyx width.

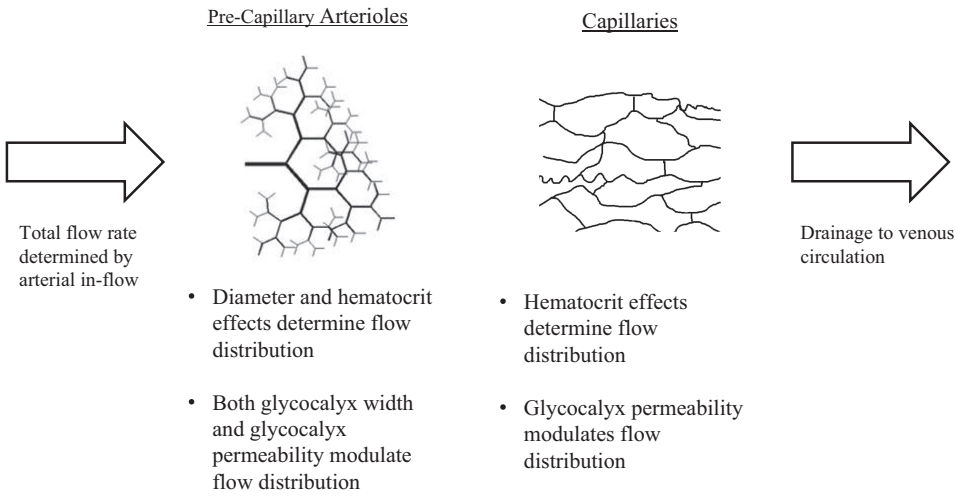

Fig. 6. Summary of findings. Our simulations concern the distribution of blood flow and RBCs within precapillary arterioles and capillaries. At this level of the circulation, total flow rate has already been determined by upstream arteries. At the arteriolar level (see *Flow distribution in branching arteriolar networks* and Fig. 3), both diameter and hematocrit dependencies of blood viscosity influence flow distribution. At the capillary level (see *Flow distribution at an idealized capillary bifurction* and Fig. 4), the hematocrit dependency of blood viscosity modulates flow distribution. Based on the influences of glycocalyx properties on the diameter and hematocrit dependencies of blood viscosity (see *Influences of glycocalyx properties on the determinants of blood viscosity* and Fig. 5), this suggests that both glycocalyx width and permeability modulate flow distribution at the arteriolar level, whereas glycocalyx permeability is the primary determinant at the capillary level.

given bifurcation may be unequal, making both the diameter and hematocrit dependencies of blood viscosity (see Fig. 1) important to arteriolar blood flow distribution. These results are discussed in *Flow distribution in branching arteriolar networks*. At the capillary level, daughter vessel diameters are likely to be similar at any given bifurcation, making the hematocrit dependency of blood viscosity an important determinant of capillary blood flow distribution. These results are discussed in *Flow distribution at an idealized capillary bifurcation*. Endothelial glycocalyx width influences the diameter the diameter dependency of blood viscosity (primarily important at the arteriolar level), whereas glycocalyx permeability influences the hematocrit sensitivity of blood viscosity (primarily important at the capillary level). These results are discussed in *Influence of glycocalyx properties on the determinants of blood viscosity*. Collectively, our data are consistent with perturbed capillary perfusion under conditions that increase glycocalyx permeability (10, 12, 63), consistent with the increased width of the glycocalyx at the arteriolar level relative to the capillary level (24), and suggest that the endothelial glycocalyx promotes homogenous distribution of blood flow and RBCs within the microvasculature.

The physiological implications of our simulation results are best understood in light of the knowledge that heterogeneous distribution of oxygenated blood within the microvasculature limits effective tissue oxygenation (17, 23, 22, 36). Enzymatic degradation of the glycocalyx by hyaluronidase or heparinase has been reported to acutely redistribute flow to a smaller number of capillaries at a higher hematocrit (10, 12). In addition, hyaluronidase treatment has been shown to markedly increase the heterogeneity of flow velocities in both arterioles and venules (see Fig. 1 in Ref. 10). These results support our finding that glycocalyx permeability is an important determinant of perfusion homogeneity/heterogeneity, given that the hyaluronan component of the glycocalyx is a major determinant of glycocalyx permeability (20). Furthermore, glycocalyx shedding during adenosine infusion (6) or systemic inflammation (11) has been shown to be associated with reduced oxygen extraction, as would be expected in the case of increased perfusion heterogeneity (17, 23, 22, 36). Our finding that the glycocalyx is a crucial regulator of microvascular perfusion and tissue oxygenation independently from total blood flow is consistent with these clinical and experimental observations.

Reports of impaired microvascular perfusion in diabetes further support the clinical relevance of our simulation results. Direct measurement endothelial glycocalyx properties in human diabetes reveals decreased glycocalyx width and increased glycocalyx permeability, which can be partially reversed by the diabetic medications metformin and sulodexide (7, 13). The microvascular effects reported with either enzymatic glycocalyx degradation or diabetes are also recapitulated by short-term hyperglycemia, which acutely increases vascular permeability and increases heterogeneity of capillary perfusion (63). The results of Frisbee et al. (16) are of particular interest, showing divergence of arterial perfusion and skeletal muscle fatigue resistance in the obese Zucker rat (a common animal model of type 2 diabetes) owing to impaired oxygen extraction. This effect was determined to stem from increased heterogeneity of microvascular perfusion (18), which also caused an increase in capillary hematocrit heterogeneity (consistent with the effects of enzymatic glycocalyx degradation) (9), and has been determined to contribute to peripheral vascular disease in this model (17). A reduction in the fraction of capillaries supporting RBC flux has been reported in animal models of both type 1 diabetes and type 2 diabetes (25, 37). Given the striking similarity between these profiles of altered capillary hematocrit and given that perturbed oxygen extraction during exercise has been demonstrated in human diabetes (1, 62), these data are once again consistent with our finding that the sensitivity of blood viscosity to hematocrit imparted by the glycocalyx is a crucial regulator of microvascular perfusion and tissue oxygenation independent from total blood flow.

The protective effects of the endothelial glycocalyx (54) may include promoting homogenous microvascular perfusion and thus improving tissue oxygenation. This is of clinical relevance as microvascular perfusion heterogeneity is found in sepsis (27), aging (28), diabetes (18), chronic heart failure (46), peripheral arterial disease (2), cancer (29), and pulmonary hypertension (32), among others. Our findings of microvascular perfusion heterogeneity with glycocalyx degradation are not entirely novel (10, 12). The simulations in this study are, however, the first to explicitly define a mechanism for increased microvascular perfusion heterogeneity under conditions of glycocalyx degradation (marginal energy costs of increasing hematocrit being inversely related to glycocalyx permeability). In addition, this study is also the first to our knowledge to mechanistically link glycocalyx degradation to impaired tissue oxygenation.

There are certain limitations of the analyses included in this study. The first is that the formulation of arteriolar branching used here does not necessarily represent real microvascular architecture (4, 21, 53). Specifically, the use of Murray's cube law (33) may influence our results. However, simulations using alternative power scaling laws with powers both >3 and <3 yielded qualitatively similar results to those reported here, and the formulations used here have been validated elsewhere as approximations of arteriolar branching structure in a variety of tissues (60, 61). Moreover, our simplified vascular architecture lends itself to straightforward analysis of the complex interplay between blood viscosity and microvascular architecture, the results of which can be applied to tissue-specific properties in future studies. In addition, our analysis of flow partitioning at an idealized capillary bifurcation could conceivably fail to generalize to an entire capillary network. There is ample empirical evidence, however, that the predicted alterations in capillary perfusion do in fact occur if the glycocalyx is degraded (10, 12, 63). Finally, the empirical formulation of in vivo blood viscosity used in this study was derived from measurements in the rat mesentery (45) and may not generalize to other species or vascular beds. Based on our finding that the semipermeable nature of the glycocalyx is sufficient to recapitulate key differences between the referenced in vivo and in vitro blood viscosity formulations and given the similarity of our results to previous simulation results (14, 50, 51), it appears likely that our findings represent a general property of the endothelial glycocalyx and not an organ-specific or species-specific effect. Our finding that the endothelial glycocalyx limits microvascular perfusion heterogeneity by increasing the influence of RBC-vessel wall interactions holds great promise for future mechanistic studies in a variety of disease states known to involve both glycocalyx degradation and tissue oxygenation defects.

ACKNOWLEDGMENTS

The authors acknowledge Dr. Amy Keller, Dr. Rebecca Scalzo, Dr. Judith Regensteiner, Dr. Pete Watson, Dr. Irene Schauer, and Chelsea Connon, all at the University of Colorado Anschutz Medical Campus, for the support and input during creation of this manuscript.

GRANTS

This work was supported by Colorado Clinical and Translational Sciences Institute-UL1-RR-025780 (to J. E. B. Reusch, M. Schafer, K. S. Hunter, and P. M. McClatchey), the Center for Women's Health Research (to J. E. B. Reusch), Veterans Affairs Merit Review (to J. E. B. Reusch), and the Department of Bioengineering (to P. M. McClatchey).

DISCLOSURES

No conflicts of interest, financial or otherwise, are declared by the author(s).

AUTHOR CONTRIBUTIONS

P.M.M. and J.E.R. conception and design of research; P.M.M. performed experiments; P.M.M. and M.S. analyzed data; P.M.M., M.S., K.S.H., and J.E.R. interpreted results of experiments; P.M.M. prepared figures; P.M.M. drafted manuscript; P.M.M., M.S., K.S.H., and J.E.R. edited and revised manuscript; P.M.M., M.S., K.S.H., and J.E.R. approved final version of manuscript.

REFERENCES

1. **Baldi JC, Aoina JL, Oxenham HC, Bagg W, Doughty RN.** Reduced exercise arteriovenous O_2 difference in type 2 diabetes. *J Appl Physiol* 94: 1033–1038, 2003.
2. **Bauer TA, Brass EP, Hiatt WR.** Impaired muscle oxygen use at onset of exercise in peripheral arterial disease. *J Vasc Surg* 40: 488–493, 2004.
3. **Becker BF, Chappell D, Bruegger D, Annecke T, Jacob M.** Therapeutic strategies targeting the endothelial glycocalyx: acute deficits, but great potential. *Cardiovasc Res* 87: 300–310, 2010.
4. **Binder KW, Murfee WL, Song J, Laughlin MH, Price RJ.** Computational network model prediction of hemodynamic alterations due to arteriolar remodeling in interval sprint trained skeletal muscle. *Microcirculation* 14: 181–192, 2007.
5. **Borges RC, Carvalho CR, Colombo AS, da Silva Borges MP, Soriano FG.** Physical activity, muscle strength, and exercise capacity 3 months after severe sepsis and septic shock. *Intensive Care Med* 41: 1433–1444, 2015.
6. **Brands J, Spaan JA, Van den Berg BM, Vink H, VanTeeffelen JW.** Acute attenuation of glycocalyx barrier properties increases coronary blood volume independently of coronary flow reserve. *Am J Physiol Heart Circ Physiol* 298: H515–H523, 2010.
7. **Zheng J, Hasting MK, Zhang X, Coggan A, An H, Snozek D, Curci J, Mueller MJ.** Effect of sulodexide on endothelial glycocalyx and vascular permeability in patients with type 2 diabetes mellitus. *Diabetologia* 53: 2646–2655, 2010.
8. **Burke-Gaffney A, Evans TW.** Lest we forget the endothelial glycocalyx in sepsis. *Crit Care* 16: 121, 2012.
9. **Butcher JT, Stanley SC, Brooks SD, Chantler PD, Wu F, Frisbee JC.** Impact of increased intramuscular perfusion heterogeneity on skeletal muscle microvascular hematocrit in the metabolic syndrome. *Microcirculation* 21: 677–687, 2014.
10. **Cabrales P, Vázquez BYS, Tsai AG, Intaglietta M.** Microvascular and capillary perfusion following glycocalyx degradation. *J Appl Physiol* 102: 2251–2259, 2007.
11. **Chappell D, Westphal M, Jacob M.** The impact of the glycocalyx on microcirculatory oxygen distribution in critical illness. *Curr Opin Anesthesiol* 22: 155–162, 2009.
12. **Desjardins C, Duling BR.** Heparinase treatment suggests a role for the endothelial cell glycocalyx in regulation of capillary hematocrit. *Am J Physiol Heart Circ Physiol* 258: H647–H654, 1990.
13. **Eskens BJ, Zuurbier CJ, van Haare J, Vink H, van Teeffelen JW.** Effects of two weeks of metformin treatment on whole-body glycocalyx barrier properties in *db*/*db* mice. *Cardiovasc Diabetol* 12: 175, 2013.
14. **Feng J, Weinbaum S.** Lubrication theory in highly compressible porous media: the mechanics of skiing, from red cells to humans. *J Fluid Mechanics* 422: 281–317, 2000.
15. **Fleg JL, Lakatta EG.** Role of muscle loss in the age-associated reduction in $V_{O_2\,max}$. *J Appl Physiol* 65: 1147–1151, 1988.
16. **Frisbee JC, Goodwill AG, Butcher JT, Olfert IM.** Divergence between arterial perfusion and fatigue resistance in skeletal muscle in the metabolic syndrome. *Exp Physiol* 96: 369–383, 2011.
17. **Frisbee JC, Goodwill AG, Frisbee SJ, Butcher JT, Wu F, Chantler PD.** Microvascular perfusion heterogeneity contributes to peripheral vascular disease in metabolic syndrome. *J Physiol* 594: 2233–2243, 2016.
18. **Frisbee JC, Wu F, Goodwill AG, Butcher JT, Beard DA.** Spatial heterogeneity in skeletal muscle microvascular blood flow distribution is increased in the metabolic syndrome. *Am J Physiol Regul Integr Comp Physiol* 301: R975–R986, 2011.

19. **Hambrecht R, Fiehn E, Weigl C, Gielen S, Hamann C, Kaiser R, Yu J, Adams V, Niebauer J, Schuler G.** Regular physical exercise corrects endothelial dysfunction and improves exercise capacity in patients with chronic heart failure. *Circulation* 98: 2709–2715, 1998.
20. **Henry CB, Duling BR.** Permeation of the luminal capillary glycocalyx is determined by hyaluronan. *Am J Physiol Heart Circ Physiol* 277: H508–H514, 1999.
21. **Huo Y, Kassab GS.** Intraspecific scaling laws of vascular trees. *J Roy Soc Interface* 9: 190–200, 2012.
22. **Jespersen SN, Østergaard L.** The roles of cerebral blood flow, capillary transit time heterogeneity, and oxygen tension in brain oxygenation and metabolism. *J Cereb Blood Flow Metab* 32: 264–277, 2012.
23. **Kalliokoski KK, Knuuti J, Nuutila P.** Blood transit time heterogeneity is associated to oxygen extraction in exercising human skeletal muscle. *Microvasc Res* 67: 125–132, 2004.
24. **Kim S, Kong RL, Popel AS, Intaglietta M, Johnson PC.** Temporal and spatial variations of cell-free layer width in arterioles. *Am J Physiol Heart Circ Physiol* 293: H1526–H1535, 2007.
25. **Kindig CA, Sexton WL, Fedde MR, Poole DC.** Skeletal muscle microcirculatory structure and hemodynamics in diabetes. *Respir Physiol* 111: 163–175, 1998.
26. **Kondo N, Nomura M, Nakaya Y, Ito S, Ohguro T.** Association of inflammatory marker and highly sensitive C-reactive protein with aerobic exercise capacity, maximum oxygen uptake and insulin resistance in healthy middle-aged volunteers. *Circ J* 69: 452–457, 2005.
27. **Lam C, Tyml K, Martin C, Sibbald W.** Microvascular perfusion is impaired in a rat model of normotensive sepsis. *J Clin Invest* 94: 2077, 1994.
28. **Levin DL, Buxton RB, Spiess JP, Arai T, Balouch J, Hopkins SR.** Effects of age on pulmonary perfusion heterogeneity measured by magnetic resonance imaging. *J Appl Physiol* 102: 2064–2070, 2007.
29. **Maeda H, Wu J, Sawa T, Matsumura Y, Hori K.** Tumor vascular permeability and the EPR effect in macromolecular therapeutics: a review. *J Control Release* 65: 271–284, 2000.
30. **Mathieu-Costello O, Hoppeler H, Weibel ER.** Capillary tortuosity in skeletal muscles of mammals depends on muscle contraction. *J Appl Physiol* 66: 1436–1442, 1989.
31. **Milosevic MF, Fyles AW, Hill RP.** The relationship between elevated interstitial fluid pressure and blood flow in tumors: a bioengineering analysis. *Int J Radiat Oncol Biol Phys* 43: 1111–1123, 1999.
32. **Mohsenifar Z, Jasper AC, Koerner, SK.** Relationship between oxygen uptake and oxygen delivery in patients with pulmonary hypertension. *Am Rev Respir Dis* 138(1), 69–73, 1988.
33. **Murray CD.** The physiological principle of minimum work applied to the angle of branching of arteries. *J Gen Physiol* 9: 835–841, 1926.
34. **Neves FM, Meneses GC, Sousa NE, Menezes RR, Parahyba MC, Martins AM, Libório AB.** Syndecan-1 in acute decompensated heart failure-association with renal function and mortality. *Circ J* 79: 1511–1519, 2015
35. **O'Leary VB, Marchetti CM, Krishnan RK, Stetzer BP, Gonzalez F, Kirwan JP.** Exercise-induced reversal of insulin resistance in obese elderly is associated with reduced visceral fat. *J Appl Physiol* 100: 1584–1589, 2006.
36. **Østergaard L, Kristiansen SB, Angleys H, Frøkiær J, Hasenkam JM, Jespersen SN, Bøtker HE.** The role of capillary transit time heterogeneity in myocardial oxygenation and ischemic heart disease. *Basic Res Cardiol* 109: 1–18, 2014.
37. **Padilla DJ, McDonough P, Behnke BJ, Kano Y, Hageman KS, Musch TI, Poole DC.** Effects of Type II diabetes on capillary hemodynamics in skeletal muscle. *Am J Physiol Heart Circ Physiol* 291: H2439–H2444, 2006.
38. **Poole DC, Copp SW, Ferguson SK, Musch TI.** Skeletal muscle capillary function: contemporary observations and novel hypotheses. *Exp Physiol* 98: 1645–1658, 2013.
39. **Poole DC, Mathieu-Costello O, West JB.** Capillary tortuosity in rat soleus muscle is not affected by endurance training. *Am J Physiol Heart Circ Physiol* 256: H1110–H1116, 1989.
40. **Pries AR, Ley K, Claassen M, Gaehtgens P.** Red cell distribution at microvascular bifurcations. *Microvasc Res* 38: 81–101, 1989.
41. **Pries AR, Neuhaus D, Gaehtgens P.** Blood viscosity in tube flow: dependence on diameter and hematocrit. *Am J Physiol Heart Circ Physiol* 263: H1770–H1778, 1992.
42. **Pries AR, Secomb TW.** Microvascular blood viscosity in vivo and the endothelial surface layer. *Am J Physiol Heart Circ Physiol* 289: H2657–H2664, 2005.
43. **Pries AR, Secomb TW.** Rheology of the microcirculation. *Clin Hemorheol Microcirc* 29: 143–148, 2003.
44. **Pries AR, Secomb TW, Gaehtgens P, Gross JF.** Blood flow in microvascular networks. Experiments and simulation. *Circ Res* 67: 826–834, 1990.
45. **Pries AR, Secomb TW, Gessner T, Sperandio MB, Gross JF, Gaehtgens P.** Resistance to blood flow in microvessels in vivo. *Circ Res* 75: 904–915, 1994.
46. **Quitter F, Figulla HR, Ferrari M, Pernow J, Jung C.** Increased arginase levels in heart failure represent a therapeutic target to rescue microvascular perfusion. *Clin Hemorheol Microcirc* 54: 75–85, 2013.
47. **Reitsma S, Slaaf DW, Vink H, van Zandvoort MA, oude Egbrink MG.** The endothelial glycocalyx: composition, functions, and visualization. *Pflügers Arch* 454: 345–359, 2007.
48. **Reusch JE, Bridenstine M, Regensteiner JG.** Type 2 diabetes mellitus and exercise impairment. *Rev Endocr Metab Disord* 14: 77–86, 2013.
49. **Richardson TE, Kindig CA, Musch TI, Poole DC.** Effects of chronic heart failure on skeletal muscle capillary hemodynamics at rest and during contractions. *J Appl Physiol* 95: 1055–1062, 2003.
50. **Secomb TW, Hsu R, Pries AR.** A model for red blood cell motion in glycocalyx-lined capillaries. *Am J Physiol Heart Circ Physiol* 274: H1016–H1022, 1998.
51. **Secomb TW, Hsu R, Pries AR.** Motion of red blood cells in a capillary with an endothelial surface layer: effect of flow velocity. *Am J Physiol Heart Circ Physiol* 281: H629–H636, 2001.
52. **Secomb TW, Pries AR.** Blood viscosity in microvessels: experiment and theory. *Comptes Rendus Physique* 14: 470–478, 2013.
53. **Sriram K, Intaglietta M, Tartakovsky DM.** Hematocrit dispersion in asymmetrically bifurcating vascular networks. *Am J Physiol Heart Circ Physiol* 307: H1576–H1586, 2014.
54. **VanTeeffelen JW, Brands J, Stroes ES, Vink H.** Endothelial glycocalyx: sweet shield of blood vessels. *Trends Cardiovasc Med* 17: 101–105, 2007.
55. **Warnke KC, Skalak TC.** Leukocyte plugging in vivo in skeletal muscle arteriolar trees. *Am J Physiol Heart Circ Physiol* 262: H1149–H1155, 1992.
56. **Weinbaum S, Tarbell JM, Damiano ER.** The structure and function of the endothelial glycocalyx layer. *Annu Rev Biomed Eng* 9: 121–167, 2007.
57. **Wiederhielm CA, Woodbury JW, Kirk S, Rushmer RF.** Pulsatile pressures in the microcirculation of frog's mesentery. *Am J Physiol Legacy Content* 207: 173–176, 1964.
58. **Williamson KA, Hamilton A, Reynolds JA, Sipos P, Crocker I, Stringer SE, Alexander YM.** Age-related impairment of endothelial progenitor cell migration correlates with structural alterations of heparan sulfate proteoglycans. *Aging Cell* 12: 139–147, 2013.
59. **Wilson JR, Martin JL, Schwartz D, Ferraro N.** Exercise intolerance in patients with chronic heart failure: role of impaired nutritive flow to skeletal muscle. *Circulation* 69: 1079–1087, 1984.
60. **Zamir M.** Arterial branching within the confines of fractal L-system formalism. *J Gen Physiol* 118: 267–276, 2001.
61. **Zamir M, Medeiros JA.** Arterial branching in man and monkey. *J Gen Physiol* 79: 353–360, 1982.
62. **Zheng J, Hasting MK, Zhang X, Coggan A, An H, Snozek D, Curci J, Mueller MJ.** A pilot study of regional perfusion and oxygenation in calf muscles of individuals with diabetes with a noninvasive measure. *J Vasc Surg* 59: 419–426, 2014.
63. **Zuurbier CJ, Demirci C, Koeman A, Vink H, Ince C.** Short-term hyperglycemia increases endothelial glycocalyx permeability and acutely decreases lineal density of capillaries with flowing red blood cells. *J Appl Physiol* 99: 1471–1476, 2005.